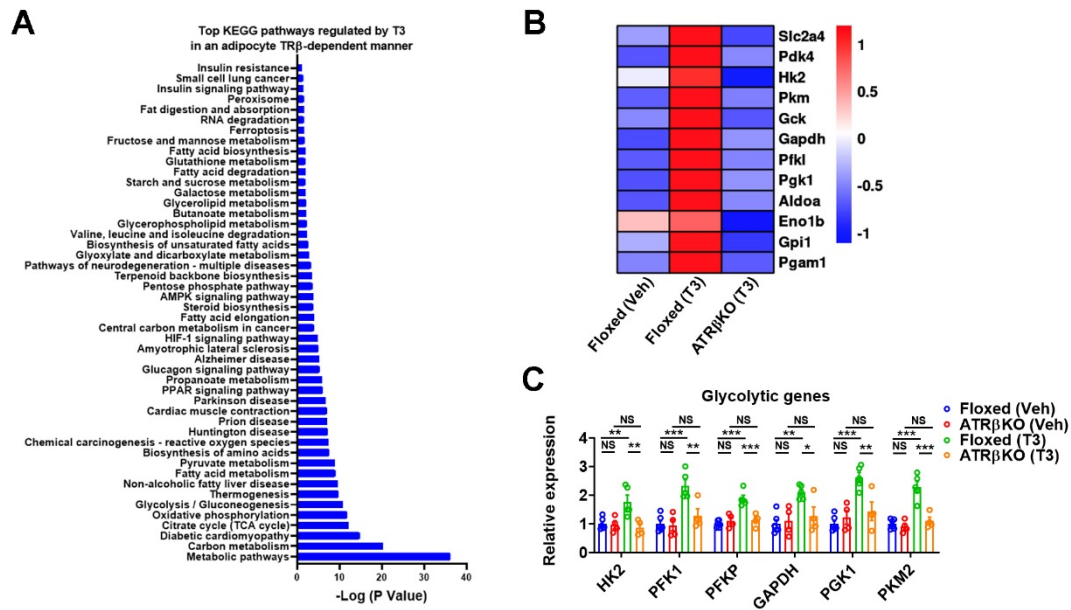


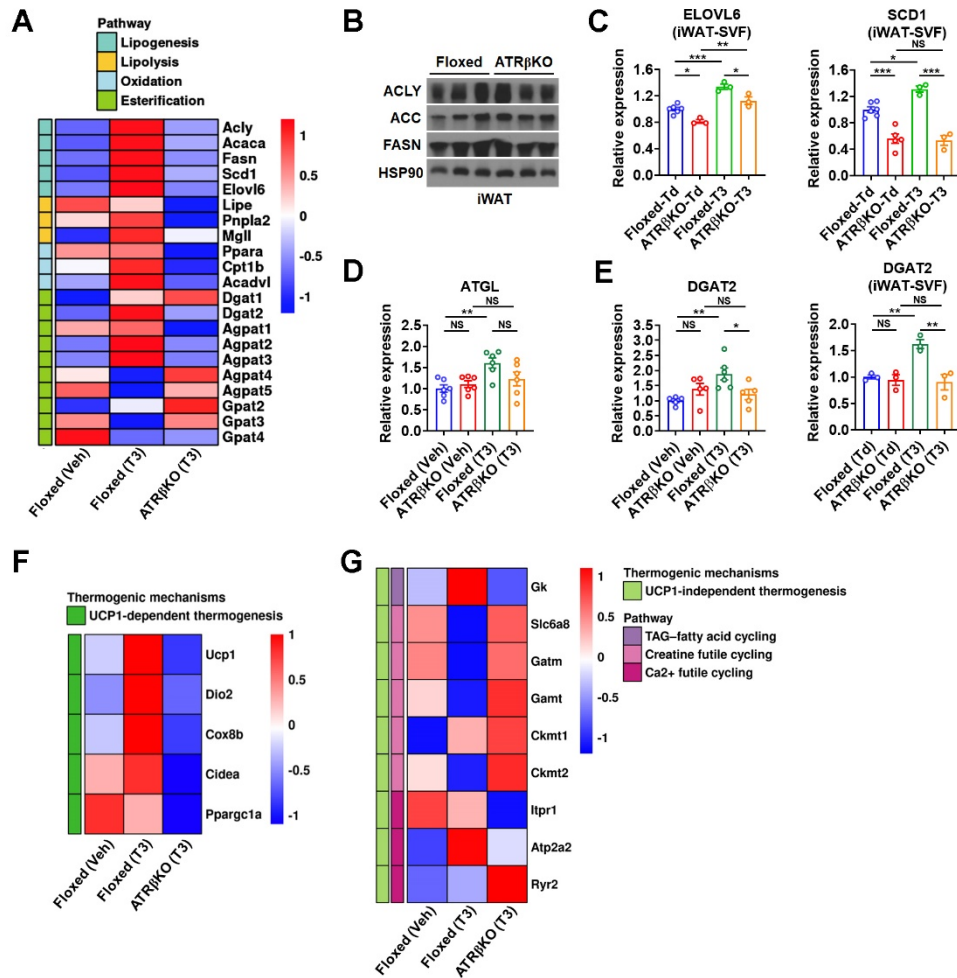
Supplementary Figure 1. T3 affects systemic metabolic homeostasis.

A: Schematic illustration of MMI and T3 administration schemes to obtain hypothyroid (MMI) mice and T3 treated (MMI+T3) mice. **B:** Glucose tolerance test (GTT) (left) and the corresponding AUC (right) of MMI and MMI+T3 mice ($n = 10$). **C** and **D:** Representative images of H&E staining of the iWAT and eWAT (**C**) and immunofluorescence (IF) staining of UCP1 of the iWAT (**D**) from MMI and MMI+T3 mice. Scale bars: 100 μm (**C**), 20 μm (**D**). **E:** Relative mRNA expression of indicated genes in iWAT of MMI and MMI+T3 mice ($n = 4-6$). **F** and **G:** Body weight (BW) of ATR β KO (**F**, $n = 9$) and ATR α KO (**G**, $n = 6-7$) mice. **H:** Representative H&E staining images of iWAT from Floxed and ATR α KO mice treated with Vehicle (Veh) or T3. Scale bars: 100 μm . **I** and **J:** Oxygen consumption (VO $_2$) (**I**, left) and energy expenditure (EE) (**J**, left) in Floxed and ATR β KO mice during the day/night cycles. Average VO $_2$ rate (**I**, right) and EE value (**J**, right) in Floxed and ATR β KO mice during the day and night, respectively ($n = 6-7$). Data are presented as mean \pm SEM. Statistical significance was determined by Student's t -test for panel **B**, **E-G**, **I** and **J**. * $p < 0.05$, ** $p < 0.01$ and *** $p < 0.001$. NS, not significant.



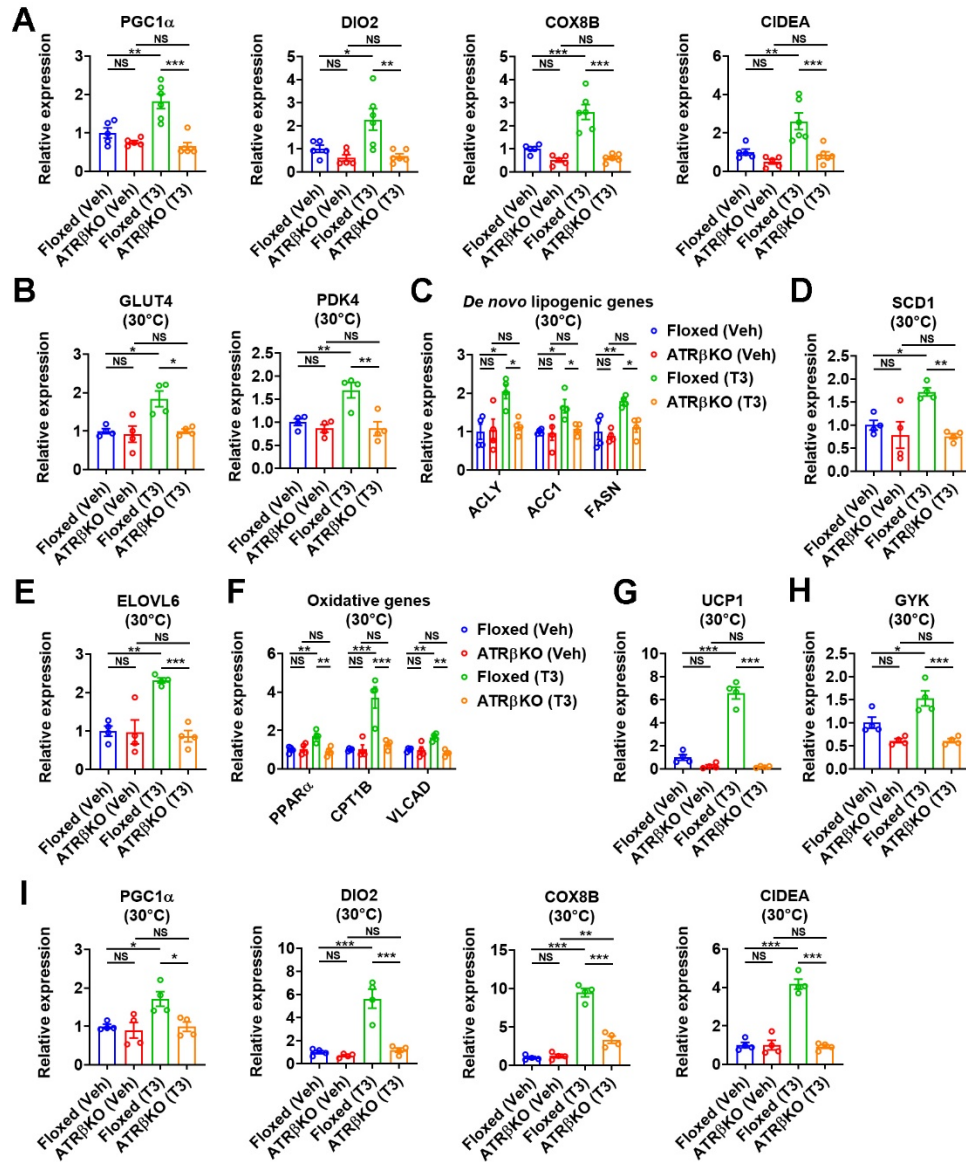
Supplementary Figure 2. TR β mediates T3 action on glucose usage in iWAT.

A: Top KEGG pathways regulated by T3 in an adipocyte TR β -dependent manner. **B:** Heatmap illustrating the expression profile of genes involved in glucose uptake and usage in the iWAT of Floxed and ATR β KO mice treated with Veh or T3. **C:** Relative mRNA expression of glycolytic genes in the iWAT of Floxed and ATR β KO mice treated with Veh or T3 ($n = 4-6$). Data are presented as mean \pm SEM. Statistical significance was determined by two-way ANOVA with Tukey's multiple comparisons test for panel C. A significant genotype-by-treatment interaction was observed for the mRNA levels of glycolytic genes (C). * $p < 0.05$, ** $p < 0.01$ and *** $p < 0.001$. NS, not significant.



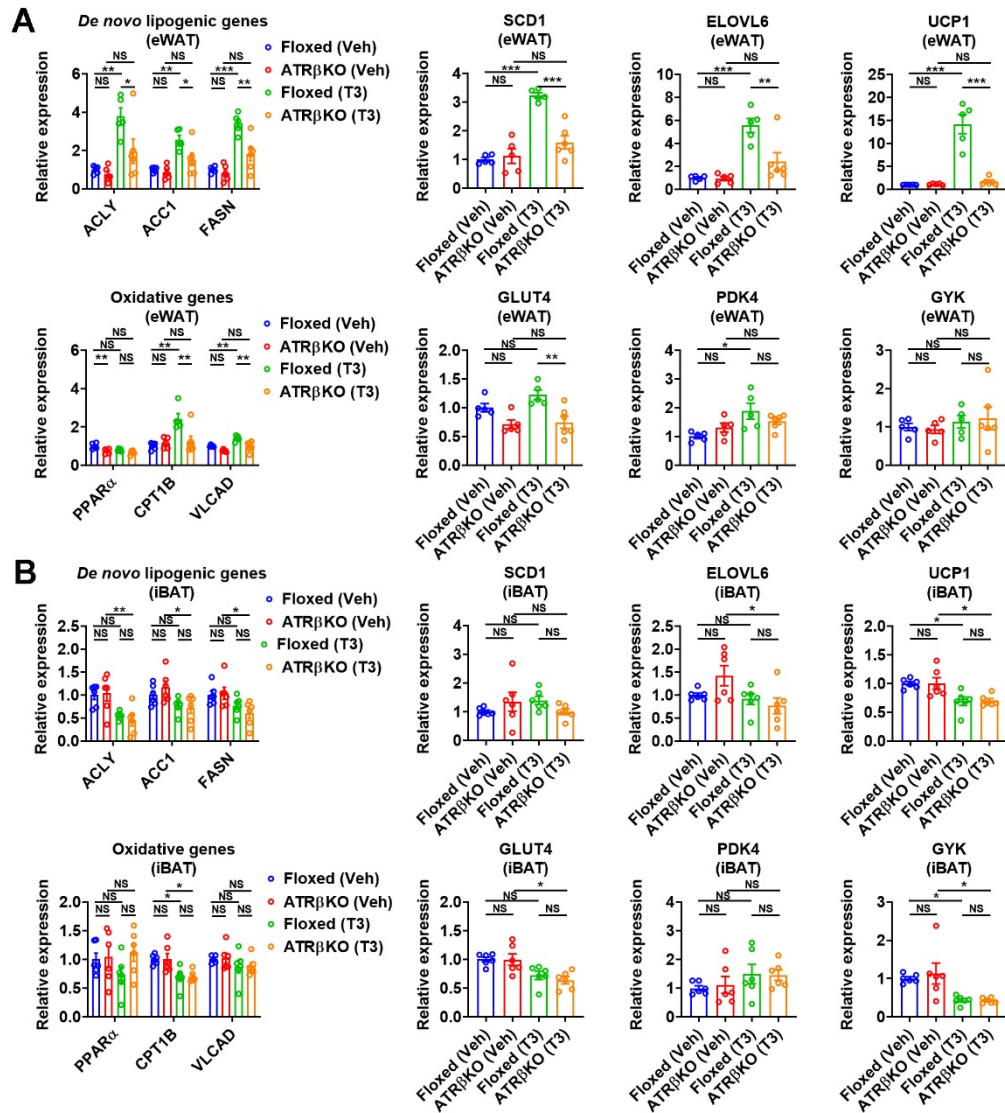
Supplementary Figure 3. TR β mediates T3 action on lipid metabolism and energy dissipation in iWAT.

A: Heatmap illustrating the expression profile of genes involved in lipid metabolism in the iWAT of Floxed and ATR β KO mice treated with Veh or T3. **B:** Western blots of ACLY, ACC, and FASN in the iWAT of Floxed and ATR β KO mice. **C:** Relative mRNA expression of ELOVL6 and SCD1 in iWAT-SVF-derived adipocytes from Floxed and ATR β KO mice in the presence or absence of T3 ($n = 3-6$). **D:** Relative mRNA expression of ATGL ($D, n = 6$) in the iWAT of Floxed and ATR β KO mice treated with Veh or T3. **E:** Relative mRNA expression of DGAT2 in the iWAT of Floxed and ATR β KO mice treated with Veh or T3 (left, $n = 5-6$) and in iWAT-SVF-derived adipocytes from Floxed and ATR β KO mice in the presence or absence of T3 (right, $n = 3$). **F** and **G:** Heatmap depicting the expression profile of genes involved in UCP1-dependent thermogenesis (**F**) and UCP1-independent thermogenic pathways, including TAG-FA cycling, creatine futile cycling, and Ca²⁺ futile cycling (**G**) in the iWAT of Floxed and ATR β KO mice treated with Vehicle or T3. Data are presented as mean \pm SEM. Statistical significance was determined by two-way ANOVA with Tukey's multiple comparisons test for panel **C-E**. A significant genotype-by-treatment interaction was observed for the mRNA levels of SCD1 (**C**) and DGAT2 (**E**). A trend for genotype-by-treatment interaction was observed for the mRNA levels of ATGL ($D, p = 0.0536$). * $p < 0.05$, ** $p < 0.01$ and *** $p < 0.001$. NS, not significant.



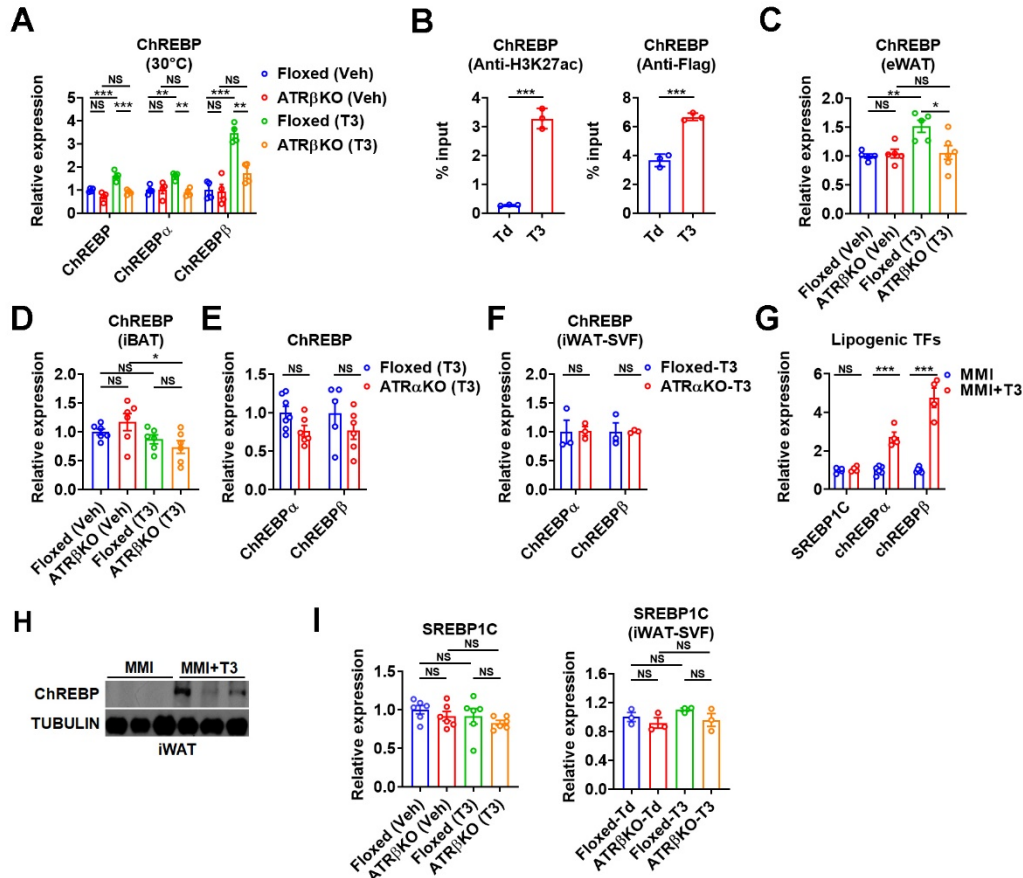
Supplementary Figure 4. The effects of T3 and loss of adipocyte TR β on gene expression in iWAT at thermoneutrality.

A: Relative mRNA expression of PGC1 α , DIO2, COX8B and CIDEA in the iWAT of Floxed and ATR β KO mice housed at room temperature (RT) treated with Veh or T3 ($n = 5-6$). B-I: Relative mRNA expression of GLUT4, PDK4 (B), *de novo* lipogenic genes (C), SCD1 (D), ELOVL6 (E), oxidative genes (F), UCP1 (G), GYK (H), PGC1 α , DIO2, COX8B and CIDEA (I) in the iWAT of Floxed and ATR β KO mice housed at 30°C treated with Veh or T3 ($n = 4$). Data are presented as mean \pm SEM. Statistical significance was determined by two-way ANOVA with Tukey's multiple comparisons test. A significant genotype-by-treatment interaction was observed for the mRNA levels of PGC1 α , DIO2, COX8B and CIDEA at RT (A), and GLUT4, PDK4 (B), ACLY (C), SCD1 (D), ELOVL6 (E), PPAR α , CPT1B, VLCAD (F), UCP1 (G), GYK (H), DIO2, COX8B and CIDEA (I) at 30°C. A trend for genotype-by-treatment interaction was observed for the mRNA levels of ACC1 (C, $p = 0.0606$), FASN (C, $p = 0.0580$) and PGC1 α (I, $p = 0.0663$) at 30°C. * $p < 0.05$, ** $p < 0.01$ and *** $p < 0.001$. NS, not significant.



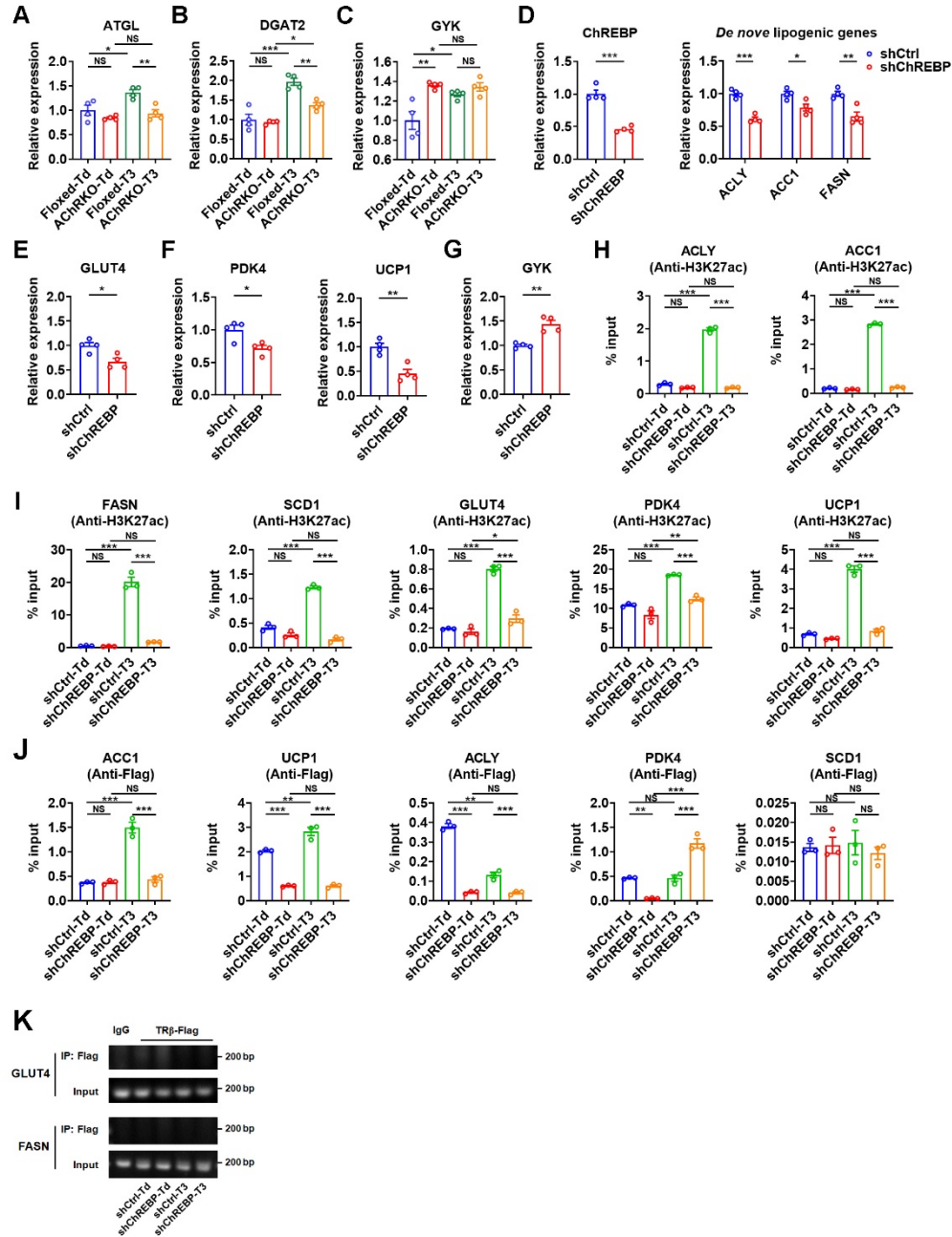
Supplementary Figure 5. Loss of adipocyte TR β has differential effects on T3-regulated gene expression in different fat depots.

A: Relative mRNA expression of *de novo* lipogenic genes, SCD1, ELOVL6, UCP1, oxidative genes, GLUT4, PDK4 and GYK in the eWAT of Floxed and ATR β KO mice treated with Veh or T3 ($n = 5-6$). **B:** Relative mRNA expression of *de novo* lipogenic genes, SCD1, ELOVL6, UCP1, oxidative genes, GLUT4, PDK4 and GYK in the iBAT of Floxed and ATR β KO mice treated with Veh or T3 ($n = 6$). Data are presented as mean \pm SEM. Statistical significance was determined by two-way ANOVA with Tukey's multiple comparisons test. A significant genotype-by-treatment interaction was observed for the mRNA levels of FASN, SCD1, ELOVL6, UCP1 and CPT1B in eWAT (**A**). A trend for genotype-by-treatment interaction was observed for the mRNA levels of ACLY (**A**, $p = 0.0904$), ACC1 (**A**, $p = 0.0747$) and PDK4 (**A**, $p = 0.0674$) in eWAT. * $p < 0.05$, ** $p < 0.01$ and *** $p < 0.001$. NS, not significant.



Supplementary Figure 6. ChREBP is controlled by the TRβ-mediated T3 signalling in iWAT.

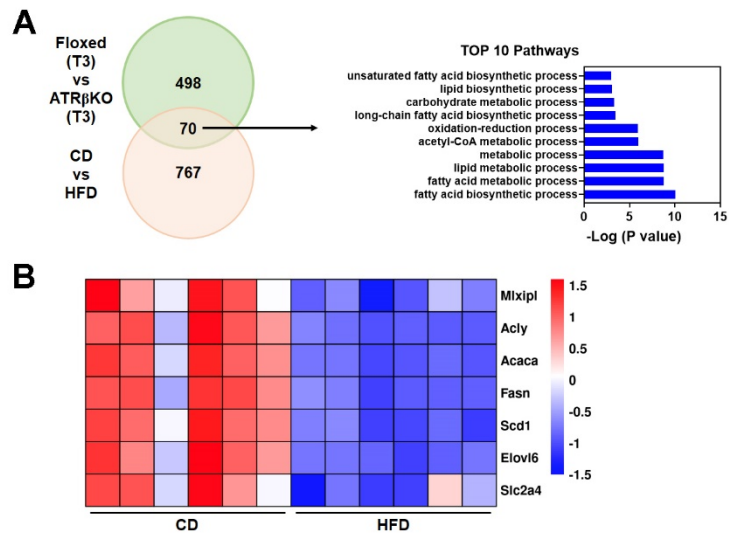
A: Relative mRNA expression of ChREBP in the iWAT of Floxed and ATRβKO mice housed at 30°C treated with Veh or T3 ($n = 4$). **B:** ChIP-PCR analysis of enrichment (percent input) of H3K27 acetylation and TRβ-Flag at the putative TRβ binding sites of the promoter region of ChREBP in iWAT-SVF-derived adipocytes in the presence or absence of T3 ($n = 3$). **C** and **D:** Relative mRNA expression of ChREBP in the eWAT (**C**, $n = 5-6$) and iBAT (**D**, $n = 6$) of Floxed and ATRβKO mice treated with Veh or T3. **E** and **F:** Relative mRNA levels of ChREBP in the iWAT of T3-treated Floxed and ATRαKO mice (**E**, $n = 5-7$) and iWAT-SVF-derived adipocytes from Floxed and ATRαKO mice in the presence of T3 (**F**, $n = 3$). **G** and **H:** Relative mRNA levels of indicated lipogenic transcription factors (TFs) (**G**, $n = 4-6$) and western blots of ChREBP (**H**) in the iWAT of MMI and MMI+T3 mice. **I:** Relative mRNA levels of SREBP1C in the iWAT of Floxed and ATRβKO mice treated with Vehicle (Veh) or T3 ($n = 6$) and in iWAT-SVF-derived adipocytes from Floxed and ATRβKO mice in the presence or absence of T3 ($n = 3$). Data are presented as mean \pm SEM. Statistical significance was determined by Student's *t*-test for panel **B** and **E-G**, and two-way ANOVA with Tukey's multiple comparisons test for panel **A**, **C**, **D** and **I**. A significant genotype-by-treatment interaction was observed for the mRNA levels of ChREBPs in iWAT at 30°C (**A**), and ChREBP in eWAT (**C**). * $p < 0.05$, ** $p < 0.01$ and *** $p < 0.001$. NS, not significant.



Supplementary Figure 7. ChREBP mediates the T3 action on metabolic genes in iWAT.

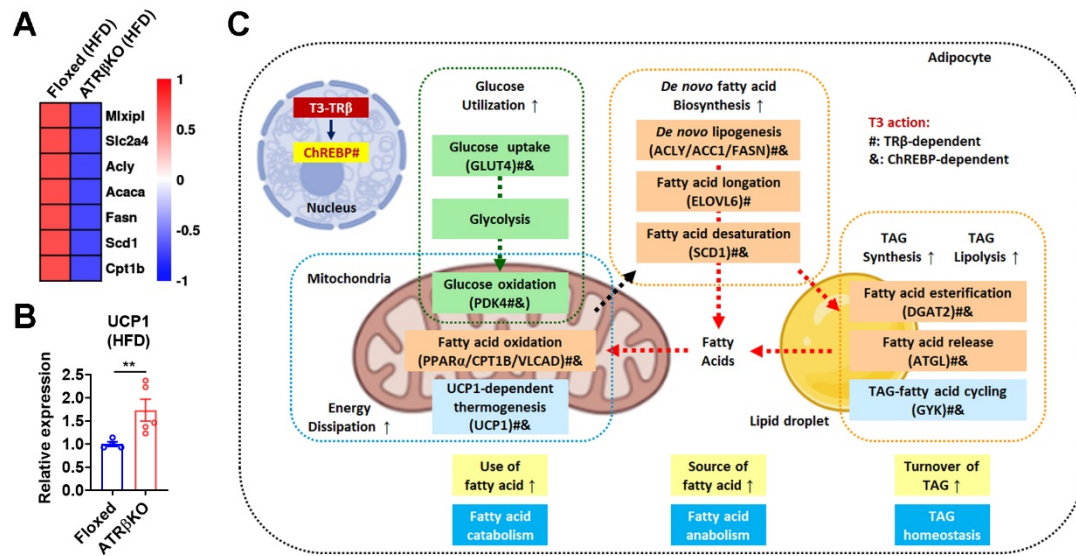
A-C: Relative mRNA expression of ATGL (A), DGAT2 (B) and GYK (C) in iWAT-SVF-derived adipocytes from Floxed and AChRKO mice in the presence or absence of T3 ($n = 4$). D-G: Relative mRNA expression of ChREBP, *de novo* lipogenic genes (D), GLUT4 (E), PDK4, UCP1 (F) and GYK (G) in iWAT-SVF-derived adipocytes infected with the shRNA lentivirus of ChREBP ($n = 4$). H and I: ChIP-PCR analysis of enrichment (percent input) of H3K27 acetylation at the putative TRβ binding sites of the promoter region of ACLY, ACC1 (H), FASN, SCD1, GLUT4, PDK4 and UCP1 (I) in iWAT-SVF-derived adipocytes infected with the shRNA lentivirus of ChREBP in the presence or absence of T3 ($n = 3$). J: ChIP-PCR analysis of TRβ-Flag recruitment (percent input) at the putative TRβ binding sites of the promoter region of ACC1, UCP1, ACLY, PDK4 and SCD1 in iWAT-SVF-derived adipocytes infected with the shRNA lentivirus of ChREBP in the presence or

absence of T3 ($n = 3$). *K*: Agarose gel electrophoresis of PCR products from ChIP-PCR analysis of TR β -Flag recruitment at the putative TR β binding sites of the promoter region of GLUT4 and FASN in iWAT-SVF-derived adipocytes infected with the shRNA lentivirus of ChREBP in the presence or absence of T3. Data are presented as mean \pm SEM. Statistical significance was determined by two-way ANOVA with Tukey's multiple comparisons test for panel *A-C* and *H-J*, and Student's *t*-test for panel *D-G*. A significant genotype-by-treatment interaction was observed for the mRNA levels of DGAT2 (*B*) and GYK (*C*). A trend for genotype-by-treatment interaction was observed for the mRNA levels of ATGL (*A*, $p = 0.0846$). A significant ChREBP knockdown-by-treatment interaction was observed for the enrichment of H3K27 acetylation for promoter of ACLY, ACC1 (*H*), FASN, SCD1, GLUT4, PDK4 and UCP1 (*I*). $*p < 0.05$, $**p < 0.01$ and $***p < 0.001$. NS, not significant.



Supplementary Figure 8. Ablation of adipocyte TR β mimics the HFD effects on glucose uptake and *de novo* FA synthesis in iWAT.

A: Venn diagram illustrating commonalities and differences between downregulated genes in the iWAT of ATR β KO mice in response to T3 treatment and downregulated genes in the iWAT of mice upon HFD feeding (left). GO analysis of the overlapped 70 genes (right). *B*: Heatmap depicting the expression profile of indicated genes involved in glucose uptake and *de novo* FA synthesis in the iWAT of Control diet (CD)-fed and HFD-fed mice based on the analysis of the RNA-seq data reported by Tiziana Caputo et al. (GSE132885).



Supplementary Figure 9. Ablation of adipocyte TR β worsens HFD-induced metabolic defects.

A: Heatmap depicting the expression profile of ChREBP, GLUT4, genes involved in FA anabolism and catabolism in the iWAT from Floxed and ATR β KO mice after HFD feeding. **B:** Relative mRNA expression of UCP1 in the iWAT of HFD-fed Floxed and ATR β KO mice ($n = 4-5$). **C:** Schematic model of the role of T3 on glucose and lipid metabolism in adipocytes. T3 action: #, TR β -dependent; &, ChREBP-dependent. Data are presented as mean \pm SEM. Statistical significance was determined by Student's t -test for panel B. * $p < 0.05$, ** $p < 0.01$ and *** $p < 0.001$. NS, not significant.